

## Cation ordering in Co-Mg olivine solid-solution series

MICHIHIRO MIYAKE

Department of Applied Chemistry, Faculty of Engineering, Yamanashi University, Takeda, Kofu 400, Japan

HAJIME NAKAMURA, \* HIRONAO KOJIMA

Institute of Inorganic Synthesis, Faculty of Engineering, Yamanashi University, Takeda, Kofu 400, Japan

FUMIYUKI MARUMO

Research Laboratory of Engineering Materials, Tokyo Institute of Technology, Nagatsuta, Midori, Yokohama 227, Japan

### ABSTRACT

Five Co-Mg olivines ( $\text{Co}_{0.23}\text{Mg}_{1.77}\text{SiO}_4$ ,  $\text{Co}_{0.4}\text{Mg}_{1.6}\text{SiO}_4$ ,  $\text{Co}_{0.92}\text{Mg}_{1.08}\text{SiO}_4$ ,  $\text{Co}_{1.45}\text{Mg}_{0.55}\text{SiO}_4$ , and  $\text{Co}_{1.76}\text{Mg}_{0.24}\text{SiO}_4$ ) and  $\text{Co}_2\text{SiO}_4$  have been systematically synthesized by a floating-zone method and investigated by X-ray diffraction methods in order to clarify the intracrystalline distribution of  $\text{Co}^{2+}$  and  $\text{Mg}^{2+}$  ions between two octahedral sites [M(1) and M(2)]. Anisotropic least-squares refinements of the structures including the cation occupancies indicate that  $\text{Co}^{2+}$  ions are strongly concentrated on the smaller M(1) octahedral sites over the Co-Mg olivine solid-solution series. The octahedral distortion for the M(1) site shows a larger increase with increasing  $\text{Co}^{2+}$  content, whereas that for the M(2) site shows a small increase. The intracrystalline distribution coefficient,  $K_D = [\text{Mg}_{\text{M(2)}}\text{Co}_{\text{M(1)}}]/[\text{Mg}_{\text{M(1)}}\text{Co}_{\text{M(2)}}]$ , attains a maximum of  $K_D \approx 5.4$  at about 50 mol%  $\text{Co}_2\text{SiO}_4$ .

### INTRODUCTION

Inter- and intracrystalline partitioning behavior of  $3d$  transition-metal ions in the olivines is of great geological, geophysical, and geochemical significance because the olivines are important constituents of the upper mantle. In Fe-Mg olivine solid-solution series, it was clarified that the larger  $\text{Fe}^{2+}$  ions preferentially occupy the smaller M(1) octahedral sites (Finger, 1970; Finger and Virgo, 1971; Brown and Prewitt, 1973; Smyth and Hazen, 1973; Wenk and Raymond, 1973). These results, based on X-ray data, are supported by Mössbauer (Bush et al., 1970; Finger and Virgo, 1971; Virgo and Hafner, 1972) and crystal-field studies (Walsh et al., 1974, 1976). The refined cation occupancies on the two octahedral sites for  $\text{Ni}_{1.03}\text{Mg}_{0.97}\text{SiO}_4$  (Rajamani et al., 1975),  $\text{Ni}_{1.16}\text{Mg}_{0.84}\text{SiO}_4$  (Bish, 1981) and  $\text{Co}_{1.1}\text{Mg}_{0.9}\text{SiO}_4$  olivines (Ghose and Wan, 1974) revealed that both  $\text{Ni}^{2+}$  and  $\text{Co}^{2+}$  ions are strongly enriched on the M(1) octahedral sites. These results, based on X-ray data, are consistent with predictions by Burns (1970) and Walsh et al. (1974, 1976).

The intracrystalline distribution coefficients,  $K_D = [\text{Mg}_{\text{M(2)}}\text{Co}_{\text{M(1)}}]/[\text{Mg}_{\text{M(1)}}\text{Co}_{\text{M(2)}}]$ , in Fe-Mg olivines of various composition have been reported by Finger (1970), Bush et al. (1970), Finger and Virgo (1971), Virgo and Hafner (1972), Brown and Prewitt (1973), Wenk and Raymond (1973), Smyth and Hazen (1973), and Aikawa et al. (1985). However, a significant correlation of  $K_D$  with composition could not be found among them, because natural Fe-Mg olivines that crystallized under different cooling

conditions were utilized in the structural studies. It is probably possible to find the correlation of  $K_D$  with composition in the Fe-Mg olivine solid-solution series with the same cooling histories. The correlations of  $K_D$  with composition were also unknown in the Ni-Mg and Co-Mg olivine solid-solution series. The relationship between  $K_D$  and composition in the olivines is of great importance for determination of the factors controlling the site preference of  $3d$  transition-metal ions.

In the present study, five Co-Mg olivines ( $\text{Co}_{0.23}\text{Mg}_{1.77}\text{SiO}_4$ ,  $\text{Co}_{0.4}\text{Mg}_{1.6}\text{SiO}_4$ ,  $\text{Co}_{0.92}\text{Mg}_{1.08}\text{SiO}_4$ ,  $\text{Co}_{1.45}\text{Mg}_{0.55}\text{SiO}_4$ , and  $\text{Co}_{1.76}\text{Mg}_{0.24}\text{SiO}_4$ ) and  $\text{Co}_2\text{SiO}_4$  have been synthesized by a floating-zone method and investigated by X-ray diffraction in order to clarify the intracrystalline partitioning behavior of  $\text{Co}^{2+}$  ions as a function of composition. The octahedral distortions of the M(1) and M(2) sites and the intracrystalline distribution coefficients in the Co-Mg olivine solid-solution series are discussed on the basis of our results, compared with the previous results (Ghose and Wan, 1974).

### SPECIMENS

The single crystals used in this study were synthesized by the following procedures.  $\text{CoO}$ ,  $\text{MgCO}_3$ , and  $\text{SiO}_2$  were mixed in the desired proportions, and intimate mixtures were shaped into rods by a rubber-press method. Rods sintered at about  $1500^\circ\text{C}$  were set in an infrared thermal-image furnace with two halogen lamps. The single crystals were elongated along the  $a$  axis at a growth rate of 1 mm/h. Large single crystals of synthetic olivines have not been obtained in the past, since they were synthesized by a flux method. Takei et al. (1982) and Inoue et al. (1982)

\* Present address: Nihon Kogaku Co., Tokyo, Japan.

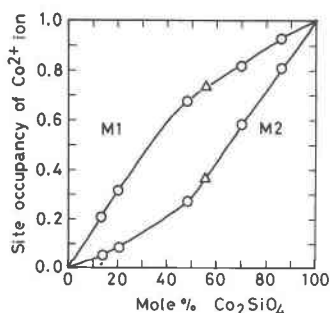


Fig. 1. Plot of site occupancies versus mol%  $\text{Co}_2\text{SiO}_4$  for Co-Mg olivine solid-solution series. Results of Ghose and Wan (1974) are shown as triangles.

first met with success in growing large and high-quality single crystals of the olivines by the Czochralski-pulling and floating-zone methods. Single crystals with dimensions 5 to 10 mm in diameter and 20 to 70 mm in length were obtained over the Co-Mg olivine solid-solution series. The colors of the obtained crystals vary from light reddish purple to dark purple with increasing  $\text{Co}^{2+}$  content.

Weissenberg photographs showed that the synthetic crystals all belong to the orthorhombic space group  $Pbnm$ . The distribution of Co and Mg atoms in the obtained crystals was examined along the  $a$  axis and the direction perpendicular to the  $a$  axis by an electron-probe microanalyser (EPMA). The EPMA technique revealed that the ratio of Co/Mg atoms is constant in the inner region of the synthesized crystals. The single crystals for intensity collection were cut down from the homogeneous regions of the rod crystals with compositions of 11.5 ( $\text{Co}_{03}$ ), 20 ( $\text{Co}_{05}$ ), 46 ( $\text{Co}_{10}$ ), 72.5 ( $\text{Co}_{15}$ ), 88 ( $\text{Co}_{18}$ ) and 100 ( $\text{Co}_{20}$ ) mol%  $\text{Co}_2\text{SiO}_4$  and were shaped into spherical crystals of about 0.15 mm in diameter. The chemical compositions of the single crystals used were quantitatively analyzed by atomic absorption spectrophotometry (Table 1).

### STRUCTURE REFINEMENTS

Intensities were measured on a Rigaku automated four-circle diffractometer with  $\text{MoK}\alpha$  radiation, monochromated with graphite, up to  $2\theta = 90^\circ$  by  $\omega$ - $2\theta$  scan technique. The scan speed was  $2.0^\circ \text{ min}^{-1}$  in  $\omega$ , and the scan was repeated three times when the total counts were less than 10 000. A scan width was determined according to

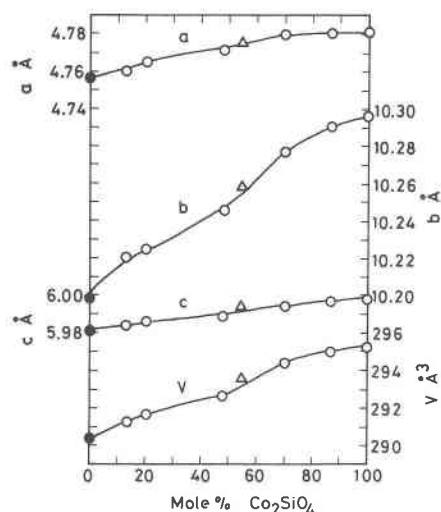


Fig. 2. Plot of cell dimensions versus mol%  $\text{Co}_2\text{SiO}_4$  for Co-Mg olivine solid-solution series. Results of Matsui and Syono (1968) and Ghose and Wan (1974) are shown as filled circles and triangles, respectively.

the formula  $(1.8 + 0.4 \tan \theta)^\circ$ . The intensities were corrected for Lorentz and polarization factors. The numbers of the collected independent intensity data satisfying the condition  $|F| > 3\sigma(|F|)$  are listed in Table 1, and these data were used for the structure refinements, where  $\sigma(|F|)$  is the standard deviation due to counting statistics.

The positional and thermal parameters including the occupancies of  $\text{Co}^{2+}$  and  $\text{Mg}^{2+}$  ions on two octahedral sites were refined with the full-matrix least-squares program LINUS (Coppens and Hamilton, 1970), starting with the positional parameters given by Ghose and Wan (1974) and Tamada et al. (1983). The occupancies,  $x_1$  and  $x_2$ , of  $\text{Co}^{2+}$  ions on the M(1) and M(2) octahedral sites were employed as parameters, and those of  $\text{Mg}^{2+}$  ions were reset by  $1 - x_1$  and  $1 - x_2$ , respectively. Corrections for isotropic secondary extinction and absorption factors were carried out in the course of the structure refinements, assuming the crystals to be spherical. The atomic scattering factors and the dispersion-correction factors for neutral atoms were taken from the *International Tables for X-ray Crystallography* (1974). Unit weights were allotted to all reflections. The  $R$  values and the positional and thermal parameters for the final anisotropic refine-

TABLE 1. Comparison between results by atomic absorption and site-refinement techniques, number of independent reflections, and  $R$  value for Co-Mg olivine solid-solution series

	$\text{Co}_{03}$	$\text{Co}_{05}$	$\text{Co}_{10}$	$\text{Co}_{15}$	$\text{Co}_{18}$	$\text{Co}_{20}$
Nutrient composition	$\text{Co}_{0.3}\text{Mg}_{1.7}\text{SiO}_4$	$\text{Co}_{0.5}\text{Mg}_{1.5}\text{SiO}_4$	$\text{Co}_{1.0}\text{Mg}_{1.0}\text{SiO}_4$	$\text{Co}_{1.5}\text{Mg}_{0.5}\text{SiO}_4$	$\text{Co}_{1.8}\text{Mg}_{0.2}\text{SiO}_4$	$\text{Co}_2\text{SiO}_4$
Atomic absorption technique	$\text{Co}_{0.23}\text{Mg}_{1.77}$	$\text{Co}_{0.40}\text{Mg}_{1.60}$	$\text{Co}_{0.92}\text{Mg}_{1.08}$	$\text{Co}_{1.45}\text{Mg}_{0.55}$	$\text{Co}_{1.76}\text{Mg}_{0.24}$	—
Site-refinement technique	$\text{Co}_{0.26}\text{Mg}_{1.74}$	$\text{Co}_{0.40}\text{Mg}_{1.60}$	$\text{Co}_{0.95}\text{Mg}_{1.05}$	$\text{Co}_{1.41}\text{Mg}_{0.59}$	$\text{Co}_{1.74}\text{Mg}_{0.26}$	—
Number of independent reflections	986	1155	1013	1063	947	1023
$R^*$	0.043	0.018	0.021	0.019	0.043	0.021
$R_w^{**}$	0.048	0.023	0.023	0.021	0.057	0.023

\*  $R = \sum |F_o| - |F_c| / \sum |F_o|$ .

\*\*  $R_w = [\sum w(|F_o| - |F_c|)^2 / \sum wF_o^2]^{1/2}$ .

TABLE 2. Positional and thermal parameters for Co-Mg olivine solid-solution series

	Co <sub>03</sub>	Co <sub>05</sub>	Co <sub>10</sub>	Co <sub>15</sub>	Co <sub>18</sub>	Co <sub>20</sub>
<b>M(1)</b>						
Co	0.208(3)*	0.316(1)	0.675(2)	0.816(2)	0.928(7)	1.0
Mg	0.792	0.684	0.325	0.184	0.072	0.0
U <sub>11</sub> **	0.0032(3)	0.0040(1)	0.0043(1)	0.0044(1)	0.0036(2)	0.0048(1)
U <sub>22</sub>	0.0074(3)	0.0063(1)	0.0062(1)	0.0061(1)	0.0076(3)	0.0068(1)
U <sub>33</sub>	0.0060(3)	0.0045(1)	0.0046(1)	0.0044(1)	0.0072(3)	0.0050(1)
U <sub>12</sub>	0.0001(2)	-0.0002(1)	-0.0002(1)	-0.0000(1)	-0.0001(2)	-0.0000(1)
U <sub>13</sub>	-0.0006(2)	-0.0005(1)	-0.0005(1)	-0.0006(1)	-0.0006(2)	-0.0006(1)
U <sub>23</sub>	-0.0008(2)	-0.0011(1)	-0.0010(1)	-0.0011(1)	-0.0011(2)	-0.0010(1)
B†	0.44	0.39	0.40	0.39	0.48	0.44
<b>M(2)</b>						
Co	0.053(3)	0.085(1)	0.278(2)	0.589(2)	0.807(7)	1.0
Mg	0.947	0.915	0.722	0.411	0.193	0.0
x‡	0.9913(2)	0.9911(1)	0.9909(1)	0.9909(1)	0.9911(2)	0.9912(1)
y	0.2771(1)	0.2770(1)	0.2767(1)	0.2765(1)	0.2765(1)	0.2765(1)
U <sub>11</sub>	0.0039(4)	0.0049(1)	0.0051(1)	0.0054(1)	0.0050(3)	0.0058(1)
U <sub>22</sub>	0.0052(4)	0.0042(1)	0.0043(1)	0.0042(1)	0.0060(3)	0.0051(1)
U <sub>33</sub>	0.0063(4)	0.0054(1)	0.0052(1)	0.0049(1)	0.0081(3)	0.0055(1)
U <sub>12</sub>	0.0003(3)	0.0003(1)	0.0002(1)	0.0002(1)	-0.0001(2)	0.0001(1)
B	0.41	0.38	0.38	0.38	0.50	0.43
<b>Si</b>						
x	0.4267(2)	0.4268(1)	0.4274(1)	0.4278(1)	0.4277(3)	0.4283(1)
y	0.0942(1)	0.0944(1)	0.0948(1)	0.0948(1)	0.0948(2)	0.0949(1)
U <sub>11</sub>	0.0021(2)	0.0029(1)	0.0032(1)	0.0034(1)	0.0027(5)	0.0035(2)
U <sub>22</sub>	0.0056(3)	0.0041(1)	0.0044(1)	0.0042(1)	0.0058(5)	0.0049(2)
U <sub>33</sub>	0.0053(3)	0.0043(1)	0.0047(1)	0.0043(1)	0.0072(5)	0.0044(2)
U <sub>12</sub>	0.0002(2)	0.0001(1)	0.0001(1)	0.0001(1)	0.0002(4)	0.0001(2)
B	0.34	0.30	0.32	0.31	0.41	0.34
<b>O(1)</b>						
x	0.7660(4)	0.7666(2)	0.7674(2)	0.7670(2)	0.7665(8)	0.7675(3)
y	0.0920(2)	0.0923(1)	0.0930(1)	0.0925(1)	0.0921(4)	0.0918(2)
U <sub>11</sub>	0.0027(6)	0.0033(2)	0.0042(3)	0.0040(3)	0.0037(11)	0.0046(5)
U <sub>22</sub>	0.0069(6)	0.0072(3)	0.0074(4)	0.0071(3)	0.0096(14)	0.0064(5)
U <sub>33</sub>	0.0065(6)	0.0058(2)	0.0060(4)	0.0061(3)	0.0088(13)	0.0062(5)
U <sub>12</sub>	-0.0001(5)	0.0005(2)	0.0006(3)	0.0003(3)	-0.0003(10)	0.0000(4)
B	0.42	0.43	0.46	0.45	0.58	0.45
<b>O(2)</b>						
x	0.2200(4)	0.2186(2)	0.2160(3)	0.2154(2)	0.2154(8)	0.2158(3)
y	0.4470(2)	0.4475(1)	0.4477(1)	0.4481(1)	0.4483(4)	0.4486(1)
U <sub>11</sub>	0.0036(6)	0.0053(2)	0.0058(4)	0.0060(3)	0.0053(12)	0.0062(5)
U <sub>22</sub>	0.0060(6)	0.0044(2)	0.0040(3)	0.0042(3)	0.0056(12)	0.0052(5)
U <sub>33</sub>	0.0074(6)	0.0067(2)	0.0066(4)	0.0070(3)	0.0104(13)	0.0069(5)
U <sub>12</sub>	-0.0001(5)	0.0001(2)	-0.0001(3)	-0.0002(3)	0.0003(10)	0.0004(4)
B	0.45	0.43	0.43	0.45	0.56	0.48
<b>O(3)</b>						
x	0.2783(3)	0.2787(1)	0.2800(2)	0.2810(2)	0.2816(6)	0.2818(2)
y	0.1633(1)	0.1635(1)	0.1640(1)	0.1640(1)	0.1641(3)	0.1641(1)
z	0.0331(2)	0.0334(1)	0.0337(1)	0.0335(1)	0.0337(5)	0.0339(2)
U <sub>11</sub>	0.0043(4)	0.0051(2)	0.0058(2)	0.0060(2)	0.0069(9)	0.0063(3)
U <sub>22</sub>	0.0072(4)	0.0068(2)	0.0073(2)	0.0077(2)	0.0088(9)	0.0079(3)
U <sub>33</sub>	0.0072(5)	0.0052(2)	0.0054(3)	0.0054(2)	0.0080(9)	0.0057(3)
U <sub>12</sub>	0.0003(4)	0.0004(1)	0.0004(2)	0.0003(2)	0.0004(7)	0.0009(3)
U <sub>13</sub>	-0.0006(4)	-0.0002(1)	-0.0004(2)	-0.0004(2)	-0.0005(7)	-0.0007(3)
U <sub>23</sub>	0.0018(4)	0.0016(1)	0.0014(2)	0.0018(2)	0.0015(8)	0.0017(3)
B	0.49	0.45	0.49	0.50	0.62	0.52

\* Numbers in parentheses are calculated standard errors and refer to the last digit quoted.

\*\*  $U_{13} = U_{23} = 0$  for M(2), Si, O(1), and O(2). Anisotropic temperature factors have the form  $\exp[-2\pi^2(U_{11}h^2a^{*2} + U_{22}k^2b^{*2} + U_{33}l^2c^{*2} + 2U_{12}hka^*b^* + 2U_{13}hla^*c^* + 2U_{23}klb^*c^*)]$ .

† B is isotropic temperature factor and calculated from the anisotropic temperature factors according to the expression  $B = 8\pi^2(U_{11} + U_{22} + U_{33})/3$ .

‡  $x = y = z = 0$  for M(1).  $z = 0.25$  for M(2), Si, O(1), and O(2).

ments for Co-Mg solid-solution series are given in Tables 1 and 2, respectively. Listings to the final observed and calculated structure factors may be ordered.<sup>1</sup>

## RESULTS AND DISCUSSION

The cation composition for each crystal estimated by the site-refinement technique is compared with that by

<sup>1</sup> To obtain structure factors, order Document AM-87-336 from the Business Office, Mineralogical Society of America, 1625 I

Street, N.W., Suite 414, Washington, D.C. 20006, U.S.A. Please remit \$5.00 in advance for the microfiche.

TABLE 3. Cell dimensions for Co-Mg olivine solid-solution series

	Co <sub>03</sub>	Co <sub>05</sub>	Co <sub>10</sub>	Co <sub>15</sub>	Co <sub>18</sub>	Co <sub>20</sub>
a	4.760(2)*	4.765(2)	4.771(1)	4.779(4)	4.780(1)	4.781(1)
b	10.221(3)	10.225(2)	10.245(1)	10.277(3)	10.290(1)	10.296(1)
c	5.984(2)	5.986(1)	5.988(1)	5.995(2)	5.997(1)	5.998(1)
V	291.13	291.65	292.69	294.44	294.97	295.25

\* Numbers in parentheses are calculated standard errors and refer to the last digit quoted.

the atomic absorption technique in Table 1. The results agree with each other within experimental error. The room-temperature olivine structures of various compositions generally exhibit isotropic temperature factors, *B*, for the M(1) and M(2) octahedral sites in the range from 0.2 to 0.45 Å<sup>2</sup> (Rajamani et al., 1975). The isotropic thermal parameters for the M(1) and M(2) octahedral sites in Co-Mg olivine solid-solution series agree fairly well with this range, as is seen in Table 2, and support the assigned octahedral site chemistry. The occupancies on two octahedral sites indicate that Co<sup>2+</sup> ions are strongly enriched on the M(1) octahedral site over the Co-Mg olivine solid-solution series. The plot of the site occupancies of Co<sup>2+</sup> ions against mol% Co<sub>2</sub>SiO<sub>4</sub> in the Co-Mg olivine solid-solution series is shown in Figure 1. The results for Co<sub>1.1</sub>Mg<sub>0.9</sub>SiO<sub>4</sub> (Ghose and Wan, 1974) are included on these curves.

The cell dimensions for the crystals determined by powder X-ray diffraction are listed in Table 3, and the plot of the cell parameters against mol% Co<sub>2</sub>SiO<sub>4</sub> in the Co-Mg olivine solid-solution series is shown in Figure 2. The *b* axis expands more than the *a* and *c* axes with increasing Co<sup>2+</sup> content and shows a drastic increase in the range from 40 to 70 mol% Co<sub>2</sub>SiO<sub>4</sub>. These changes were not found in previous studies (Matsui and Syono, 1968).

Interatomic distances (Table 4) and bond angles for each Co-Mg olivine were calculated by the program UNICS (Sakurai, 1967). The general structural details of the oliv-

ine have been thoroughly discussed by Birle et al. (1968). The mean Si-O bond lengths were found to be constant within this series and close to those in other olivines (Finger, 1970; Finger and Virgo, 1971; Brown and Prewitt, 1973; Smyth and Hazen, 1973; Wenk and Raymond, 1973; Ghose and Wan, 1974; Rajamani et al., 1975; Tamada et al., 1983). The mean M(1)-O and M(2)-O bond lengths increase with increasing Co<sup>2+</sup> content. The mean M(1)-O bond length shows a large increase below values of 50 mol% Co<sub>2</sub>SiO<sub>4</sub>, whereas the mean M(2)-O bond length shows a small increase beyond values of 50 mol% Co<sub>2</sub>SiO<sub>4</sub>.

The M(1) octahedral sites in the olivine structures are inherently smaller and more distorted than M(2) octahedral sites. The calculated octahedral distortions (Robinson et al., 1971) for the M(1) and M(2) sites of each olivine in this study are listed in Table 5. Co<sup>2+</sup> ions exhibit a strong preference for the smaller M(1) octahedral sites, and the octahedral distortion of the M(1) site increases significantly with increasing Co<sup>2+</sup> content. The increase of the octahedron distortion is particularly large below values of 50 mol% Co<sub>2</sub>SiO<sub>4</sub>. On the other hand, as Co<sup>2+</sup> ions show weak preference for the larger M(2) octahedral site, the increase of the octahedral distortion of the M(2) site is small. The variations observed in the *b* axis, the mean bond lengths of the octahedra, and the octahedral distortions are attributed to the change in site preference of Co<sup>2+</sup> ions for the M(1) and M(2) octahedral sites at about 50 mol% Co<sub>2</sub>SiO<sub>4</sub>.

TABLE 4. Interatomic distances (Å) for Co-Mg olivine solid-solution series

		Co <sub>03</sub>	Co <sub>05</sub>	Co <sub>10</sub>	Co <sub>15</sub>	Co <sub>18</sub>	Co <sub>20</sub>
		Si tetrahedron					
[1]	Si-O(1)	1.615(2)	1.619(1)	1.623(1)	1.621(2)	1.620(4)	1.622(2)
[1]	Si-O(2)	1.659(2)	1.654(1)	1.655(1)	1.655(1)	1.656(4)	1.657(2)
[2]	Si-O(3)	1.638(2)	1.637(1)	1.636(1)	1.638(1)	1.637(3)	1.636(1)
Mean	Si-O	1.638	1.637	1.638	1.638	1.638	1.638
		M(1) octahedron					
[2]	M(1)-O(1)	2.089(1)	2.090(1)	2.093(1)	2.095(1)	2.096(3)	2.093(1)
[2]	M(1)-O(2)	2.076(1)	2.080(1)	2.089(1)	2.093(1)	2.093(3)	2.092(1)
[2]	M(1)-O(3)	2.140(1)	2.145(1)	2.156(1)	2.164(1)	2.169(3)	2.170(1)
Mean	M(1)-O	2.102	2.105	2.113	2.117	2.119	2.118
		M(2) octahedron					
[1]	M(2)-O(1)	2.174(2)	2.170(1)	2.163(1)	2.173(1)	2.180(4)	2.181(2)
[1]	M(2)-O(2)	2.050(2)	2.052(1)	2.055(1)	2.064(1)	2.068(4)	2.072(2)
[2]	M(2)-O(3)	2.066(2)	2.067(1)	2.066(1)	2.066(1)	2.067(3)	2.068(1)
[2]	M(2)-O(3)	2.214(2)	2.215(1)	2.217(1)	2.223(1)	2.224(3)	2.225(1)
Mean	M(2)-O	2.131	2.131	2.131	2.136	2.138	2.140

Note: Numbers in brackets refer to the multiplicity of the bond. Numbers in parentheses are calculated standard errors and refer to the last digit quoted.

TABLE 5. Octahedral distortions and intracrystalline distribution coefficients for Co-Mg olivine solid-solution series

	Co <sub>03</sub>	Co <sub>05</sub>	Co <sub>10</sub>	Co <sub>15</sub>	Co <sub>18</sub>	Co <sub>20</sub>
$\sigma_6^2$ [M(1)]*	96.01	99.06	102.07	102.95	103.15	104.58
$\sigma_6^2$ [M(2)]	90.02	90.65	91.56	92.15	92.91	93.79
$K_D^{**}$	4.69	4.97	5.39	3.09	3.08	—

\*  $\sigma_6^2$  (oct) =  $\sum_{i=1}^{12} (\theta - 90^\circ)^2/11$  (Robinson et al., 1971).

\*\*  $K_D = \frac{[Mg_{M(2)}Co_{M(1)}]}{[Mg_{M(1)}Co_{M(2)}]}$  for the exchange reaction  $Mg_{M(1)} + Co_{M(2)} = Mg_{M(2)} + Co_{M(1)}$ .

The intracrystalline distribution coefficient,  $K_D$ , as defined earlier, was calculated for each crystal and listed in Table 5. The estimated  $K_D$  attains a maximum,  $K_D \approx 5.4$ , at about 50 mol% Co<sub>2</sub>SiO<sub>4</sub>. The maximum value is intermediate between the values for Ni-Mg (Rajamani et al., 1975; Bish, 1981) and Fe-Mg olivines (Finger, 1970; Bush et al., 1970; Finger and Virgo, 1971; Virgo and Hafner, 1972; Brown and Prewitt, 1973; Wenk and Raymond, 1973; Smyth and Hazen, 1973; Aikawa et al., 1985). This means that in the olivine structures, the preference for the M(1) octahedral site is in the order Ni<sup>2+</sup> > Co<sup>2+</sup> > Fe<sup>2+</sup>, and this order is consistent with the previous results and predictions. As the obtained  $K_D$  does not represent the equilibrium distribution between Co<sup>2+</sup> and Mg<sup>2+</sup> ions on the two octahedral sites at the temperature of synthesis, it is necessary to investigate the high-temperature structures for Co-Mg olivine in order to establish the equilibrium distribution between these cations and to estimate the free energy.

We are investigating the Fe-Mg olivine solid-solution series synthesized by the floating-zone method in order to clarify the correlation of  $K_D$  with composition. Homogeneous, large single crystals of Ni-Mg olivine could not be successfully synthesized by the floating-zone method in the region of high Ni<sup>2+</sup> content. This is ascribed to the strong preference of Ni<sup>2+</sup> ions for the M(1) octahedral site.

#### ACKNOWLEDGMENTS

We are grateful to Professor Y. Matsui of Okayama University and N. Aikawa of Osaka City University for valuable discussions. We also thank Drs. K. Tanaka, N. Kodama, and H. Naruse of Tokyo Institute of Technology for their help in the X-ray intensity measurements. The computations were carried out on an Acos 850 computer at the Computer Center of Yamanashi University.

#### REFERENCES

- Aikawa, N., Kumazawa, M., and Tokonami, M. (1985) Temperature dependence of intersite distribution of Mg and Fe in olivine and the associated change of lattice parameters. *Physics and Chemistry of Minerals*, 12, 1–8.
- Birle, J.D., Gibbs, G.V., Moore, P.B., and Smith, J.V. (1968) Crystal structures of natural olivines. *American Mineralogist*, 53, 807–824.
- Bish, D.L. (1981) Cation ordering in synthetic and natural Ni-Mg olivine. *American Mineralogist*, 66, 770–776.
- Brown, G.E., and Prewitt, C.T. (1973) High-temperature crystal chemistry of hortonolite. *American Mineralogist*, 58, 577–587.
- Burns, R.G. (1970) Mineralogical applications of crystal field theory. Cambridge University Press, Cambridge, England.
- Bush, W.R., Hafner, S.S., and Virgo, D. (1970) Some ordering of iron and magnesium at the octahedrally coordinated site in a magnesium-rich olivine. *Nature*, 227, 1339–1341.
- Coppens, P., and Hamilton, W.C. (1970) Anisotropic extinction corrections in the Zachariasen approximation. *Acta Crystallographica*, A26, 71–83.
- Finger, L.W. (1970) Fe/Mg ordering in olivines. *Carnegie Institution of Washington Year Book* 69, 302–305.
- Finger, L.W., and Virgo, D. (1971) Confirmation of Fe/Mg ordering in olivines. *Carnegie Institution of Washington Year Book* 70, 221–225.
- Ghose, S., and Wan, C. (1974) Strong site preference of Co<sup>2+</sup> in olivine, Co<sub>1.10</sub>Mg<sub>0.90</sub>SiO<sub>4</sub>. *Contributions to Mineralogy and Petrology*, 47, 131–140.
- Inoue, T., Komatsu, H., Hosoya, S., Shimizu, M., and Takei, H. (1982) Defect structures of Fe-rich olivine grown by the floating zone method. *Journal of Crystal Growth*, 57, 203–205.
- Matsui, Y., and Syono, Y. (1968) Unit cell dimensions of some synthetic olivine group solid solutions. *Geochemical Journal*, 2, 51–59.
- Rajamani, V., Brown, G.E., and Prewitt, C.T. (1975) Cation ordering in Ni-Mg olivine. *American Mineralogist*, 60, 292–299.
- Robinson, K., Gibbs, G.V., and Ribbe, P.H. (1971) Quadratic elongation: A quantitative measure of distortion in coordination polyhedra. *Science*, 172, 567–570.
- Sakurai, T. (1967) Universal Program System for Crystallographic Computations. Crystallographic Society of Japan.
- Smyth, J.R., and Hazen, R.M. (1973) The crystal structures of forsterite and hortonolite at several temperatures up to 900°C. *American Mineralogist*, 58, 588–593.
- Takei, H., Hosoya, S., and Kojima, H. (1982) Synthesis of large and high-quality single crystals of olivines, pyroxenes, pyroxenoids and ilmenites. *Ganseki Kobutsu Kosho*, S3, 73–82.
- Tamada, O., Fujino, K., and Sasaki, S. (1983) Structures and electron distributions of  $\alpha$ -Co<sub>2</sub>SiO<sub>4</sub> and  $\alpha$ -Ni<sub>2</sub>SiO<sub>4</sub> (olivine structure). *Acta Crystallographica*, B39, 692–697.
- Virgo, D., and Hafner, S.S. (1972) Temperature-dependent Mg, Fe distribution in a lunar olivine. *Earth and Planetary Science Letters*, 14, 305–312.
- Walsh, D., Donnay, G., and Donnay, J.D.H. (1974) Jahn-Teller effects in ferro-magnesian minerals: Pyroxenes and olivines. *Bulletin de la Société française de Minéralogie et de Cristallographie*, 97, 170–183.
- (1976) Ordering of transition metal ions in olivine. *Canadian Mineralogist*, 14, 149–150.
- Wenk, H.-R., and Raymond, K.N. (1973) Four new structure refinements of olivine. *Zeitschrift für Kristallographie*, 137, 86–105.

MANUSCRIPT RECEIVED SEPTEMBER 25, 1985

MANUSCRIPT ACCEPTED JANUARY 17, 1987